European Transport Research Review

ORIGINAL PAPER Open Access

Forecasts of future scenarios for airport noise based on collection and processing of web data

Marco Pretto[1*], Pietro Giannattasio[1], Michele De Gennaro[2], Alessandro Zanon[2] and Helmut Kuehnelt[2]

Abstract

Purpose: This paper presents an analysis of short-term (2025) scenarios for noise emission from civil air traffic in airport areas.

Methods: Flight movements and noise levels at a given airport are predicted using a web-data-informed methodology based on the ECAC Doc.29 model. This methodology, developed by the authors in a previous work, relies on the collection and processing of air traffic web data to reconstruct flight events to be fed into the ECAC model. Three new elements have been included: i) topographic information from digital elevation models, ii) a fleet substitution algorithm to estimate the impact of newer aircraft, and iii) a generator of flight events to simulate the expected traffic increase.

Results: The effects of these elements are observed in 2025 scenarios for the airports of London Heathrow, Frankfurt and Vienna-Schwechat. The results quantify the noise reduction from new aircraft and its increment due to the air traffic growth forecast by EUROCONTROL.

Keywords: Web data, Airport noise, ECAC Doc.29 model, Aircraft fleet, Future air traffic, Scenario analysis

1 Introduction

Since 2015, air transport in the world has been growing at a steady rate of about 7% per year, with almost 4.1 billion passengers carried by scheduled flights in 2017 [1]. Around 26% of them were served in Europe, which in the same year saw almost 11 million flights and more than 21 million flight operations, expected to increase by up to 84% by 2040 [2] also thanks to the contribution of low-cost carriers [3]. This large development, however, poses important threats such as the increase in air pollution and noise, which the EU has addressed by setting out ambitious goals in its *Flightpath 2050* [4]. According to this plan, future aircraft should lead to a reduction by 75% in CO_2 emissions, 90% in NO_x emissions and 65% in perceived noise compared to the average new aircraft in 2000. Improvements in this regard have already been accomplished in the past [5], and new practices such as aircraft electrification or biofuel adoption appear promising [6, 7].

Alongside technical developments, achieving the target of a sustainable growth also requires quantifying the effect of present and future air traffic, and this is typically carried out by using suitable prediction models. Concerning aircraft noise, a large number of models with different degrees of accuracy and complexity have been developed in the past [8]. Among them are best-practice methods, which rely on standardised datasets to enable fast computation of aircraft noise in large airport areas, and are therefore used by national aviation agencies in many countries.

Independently of the model, a key requirement for effective noise prediction is extensive information on flight movements and aircraft models, which proved difficult to retrieve up until a few years ago. In recent times, however, the introduction of ADS-B transponders has given rise to flight tracking websites such as *Flightradar24* [9] and *FlightAware* [10], which use and rearrange information from these transponders and other sources to provide the public with flight movement data in real time. The available amount of information, steadily growing thanks to EU's obligation to install ADS-B on all large aircraft by 2020 [11], is already large enough to enable statistical analysis of aircraft performance [12]. Moreover, when these data are paired

* Correspondence: pretto.marco@spes.uniud.it; marcopretto@hotmail.it
[1]Dipartimento Politecnico di Ingegneria e Architettura, University of Udine, Via delle Scienze 206, 33100 Udine, Italy
Full list of author information is available at the end of the article

with additional Internet-based sources such as aircraft model databases, it becomes possible to define flight events at an airport and use them as an input to a best-practice model. This was recently done by the present authors, who used the ECAC Doc.29 model and Internet-based data sources to compute historical noise contours at multiple European airports [13, 14].

Having demonstrated the viability of large-scale noise computation from web-based data, the present work aims to show that this approach can be used also for short-term noise forecasts. To do this, reliable predictions of future aircraft fleet composition and flight movements at a given airport are required. Two algorithms are introduced for updating to 2025 the aircraft fleet and reconstructing additional flight events due to the traffic increase expected for the same year. These algorithms are applied to historical flight movement data at three European airports, and the resulting flight events are used to predict the future airport noise contours. The present approach, upgraded to account for topographic data from digital elevation models, can be used for airports of different size and passenger volume if appropriate traffic forecasts are available.

The paper is structured as follows. Section 2 illustrates the noise computation methodology with special emphasis on how web data are used and what improvements from the previous application have been made. Then, the two algorithms used for addressing future air traffic scenarios are described. Section 3 reports the results of the application of the present approach to the airports of Heathrow, Frankfurt and Vienna-Schwechat. The conclusions of the work are drawn in Section 4.

2 Methodology

The approach described in this paper is based on the procedure of flight event reconstruction and noise computation introduced by Pretto et al. [14]. This procedure is here extended to *i)* account for the topography of the airport area and *ii)* enable an efficient prediction of the future noise levels due to variations in aircraft fleet composition and air traffic volume. The key steps of this extended approach are summarised in the flowchart of Fig. 1, aimed to support the reader in understanding the methodological steps described below.

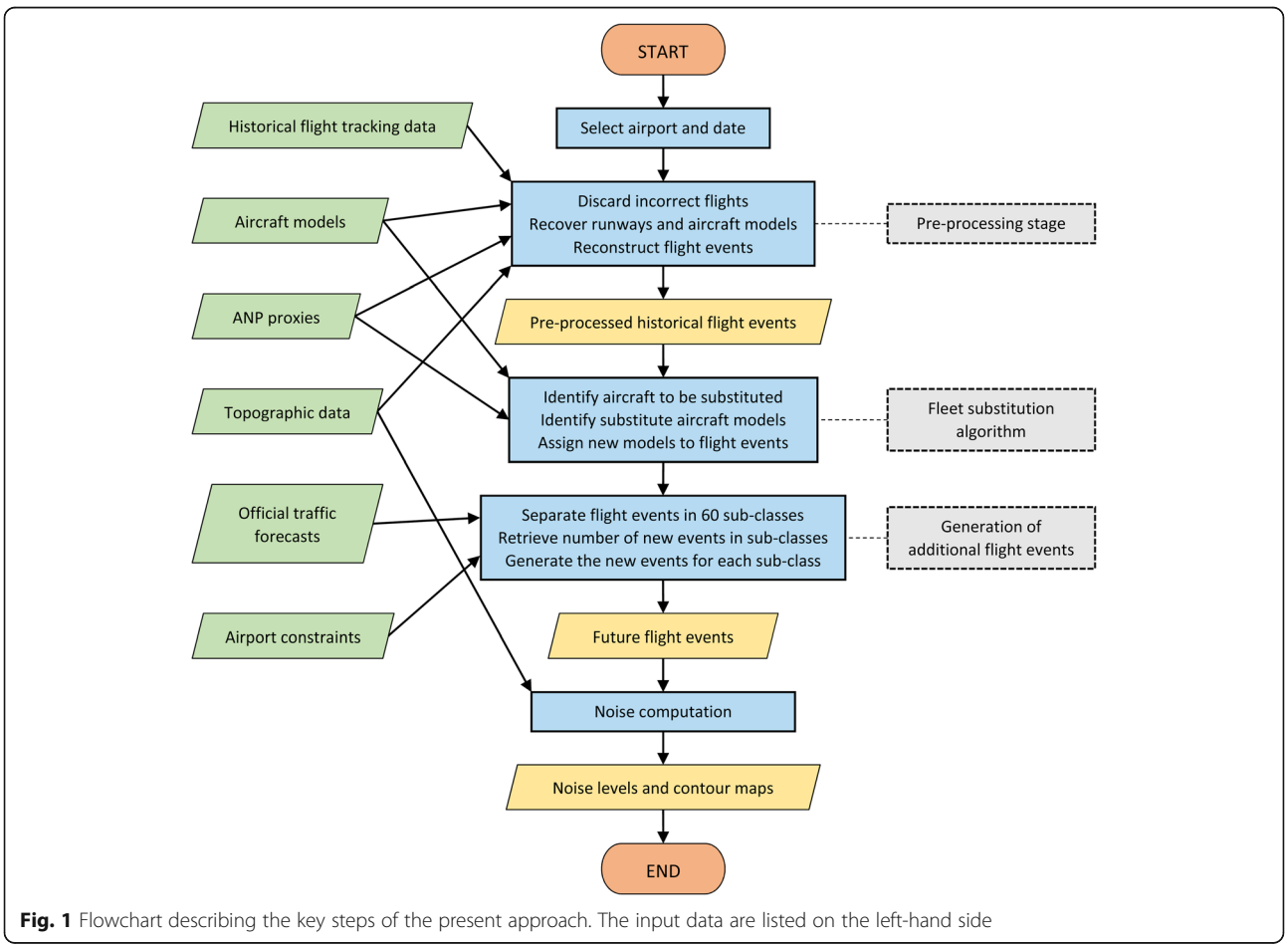

Fig. 1 Flowchart describing the key steps of the present approach. The input data are listed on the left-hand side

2.1 Summary of noise computation procedure

This subsection briefly describes the main steps that enable the computation of airport noise contours using the ECAC noise model and web-based air traffic data, with special focus on the aspects that affect the operations described from Section 2.2 onwards. The entire procedure is detailed by Pretto et al. [14].

2.1.1 ECAC Doc.29 model and ANP database

The ECAC Doc.29 model [15] is a best-practice segmentation aircraft noise prediction model that enables calculation of noise levels and contours around airports due to aircraft movements during a specified time period. At any selected airport, the model computes the desired cumulative noise metrics, such as $L_{Aeq,day}$, $L_{Aeq,night}$, L_{DEN}, and $L_{max,avg}$, by superposing the effects of single flight events, i.e. departures and arrivals. For each of them, single-event sound levels *SEL* and L_{Amax} are computed using a grid of sound receivers in the region of interest around the airport. Each of these two sound levels is computed by superposing the effects of a set of flight path segments, which represent the 3D aircraft motion over time during the event. These segments are obtained by merging the ground track, which represents the ground projection of the aircraft motion, with the flight profile, which contains information on the vertical motion above the ground track and the related flight parameters (e.g. calibrated airspeed and engine thrust).

For a single event, the ground track and the flight profile can be generated either by *analysis* of flight movement data or by *synthesis* from appropriate procedural information. In the case of flight profiles, this information consists of a series of procedural steps, which prescribe how the aircraft must be flown during a single operation (departure or arrival) in terms of speed, altitude and flap settings. These procedural steps are listed in the ANP database [16], which contains appropriate sets of flight profiles for around 140 reference aircraft models known as proxies. A flight profile is calculated using mechanical and kinematic equations that require knowledge of such profile sets, basic aircraft model features (e.g. aircraft weight) also provided by ANP, and atmospheric conditions, allowing the computation of engine thrust, height, and true and calibrated airspeeds above the ground track [17].

Once the segmented flight path for a single flight event has been obtained, the calculation of segment noise levels is performed in the ECAC noise engine by taking into account the aircraft performance inside the given segment and the location of a receiver. First, the baseline noise levels are interpolated from reference levels, known as "Noise-Power-Distance" (NPD) data and valid for a straight, infinitely long flight path flown at fixed speed, using the current values of engine thrust (power) and segment-receiver distance. Then, adjustments are made to account for atmospheric conditions, non-reference speed, position of aircraft engines, bank angle, finite segment length, sound directivity during runway movements, and reverse thrust. All segment noise levels are then superposed and *SEL* and L_{Amax} are found at a single receiver point. The process is repeated for all the receivers, thus completing the single event noise computation.

2.1.2 Integration with web-based air traffic data

The application of the ECAC model to the calculation of single event noise levels requires a complete description of the flight event. This is obtained through data collection from the Internet. The core information comes from flight tracker *Flightaware*, which was searched in June 2018 to collect raw air traffic data in nine European airports, retrieving around 11,000 flight histories. Each flight history contains the 3D locations and speeds, ordered in time and spaced by 15 s, of a certain aircraft, normally identified via its registration and ICAO type designator. All airport locations and runways were retrieved from website *OurAirports* [18], while website *Airlinerlist* [19] was used to build an offline database that associates the registration with the specific aircraft model.

As the raw flight histories were sometimes incorrect, often lacked trace of non-airborne movements, and the aircraft model was never reported explicitly, the retrieved flight data were pre-processed using the runway and aircraft information mentioned above to reconstruct the flight movement and to recover the departure/arrival runway and aircraft model. The latter was then used to enter the main ANP substitution table, which is a tool that associates a specific model with a suitable ANP proxy, thus enabling noise computation via the ECAC model. Many configurations are listed for the given model-proxy pair, which differ primarily in engine variant and weight, and hence in the noise output. Therefore, multiple values of a correction factor called "number of equivalent events", N_{eq}, are provided in the ANP tables to modify the proxy noise levels according to the specific aircraft configuration. Since the different configurations could not be retrieved, an average configuration was built for each model, and two average numbers of equivalent events (different for departures and arrivals) were assigned to the proxy. When the aircraft registration was not available, a second ANP substitution table could be used to obtain a direct ICAO designator-proxy association, as only one configuration is listed and no averaging is needed.

The reconstructed flight movements during a single departure/arrival event at the selected airport are used, together with the aircraft information, for the construction of the segmented flight path. In each flight event, the ground track is built via analysis of the 2D position

data, while the flight profile is synthesised from the ECAC procedural steps, as the time spacing between consecutive flight recordings (15 s) is too large to ensure reliable engine thrust reconstruction solely from speed and height information.

2.1.3 Generation of noise contour maps

In the original application each airport was studied separately, and all the flight events occurring on a given day were identified. For each event, the segmented flight path was built, and its contribution to airport noise was computed on a square grid of 11,881 receivers positioned every around 450 m in both x and y directions, at the same altitude as the airport reference point (ARP). Finally, the sound levels due to all flight events were superposed to obtain daily cumulative noise metrics, and hence daily noise contours in the airport area.

2.2 Noise computation accounting for topographic data

Local topography (i.e. the elevation of land surfaces around the airport) may have a non-negligible influence on the noise levels around an airport, mainly due to the elevation of the receiver points, which affects their distance from the flight path segments. Furthermore, the knowledge of local elevations allows for an improved description of the airport runways, and the reconstruction of aircraft ground movements can also be influenced. The next subsections explain how terrain elevation is accounted for in the present noise computation procedure.

2.2.1 Acquisition and implementation of topographic data

The source of topographic data for this analysis is a series of digital elevation models (DEMs) of the European territory, which includes all the airports studied. Around 1500 DEMs, each 1-degree wide in both latitude and longitude and with a 3 arc-second resolution, were downloaded from website *WebGIS* [20] and suitably post-processed in order to obtain a single elevation map for the entire Europe in the form of a 2D grid. The elevations of all ARPs and runways were computed by bilinear interpolation of grid data, and each runway was assigned a single elevation value (the one of its mid-point) and a gradient (using the elevation of its two ends). This is because the ECAC mechanical model relies on flat runways, but can account for runway gradients during a take-off. The same interpolation was performed around each airport for each receiver point involved in the noise computation procedure.

2.2.2 Line-of-sight blockage adjustment

Line-of-sight (LOS) blockage is the sound attenuation due to the presence of an obstruction along the direct propagation path between the source and the receiver. Natural structures such as mountains and hills may act as "sound shields", diffracting sound waves and thus considerably lowering noise levels behind them. The ECAC model does not account for this effect, but FAA's AEDT does through a specific LOS adjustment [21]. As the AEDT noise computation is based on the ECAC model, a straightforward implementation of this adjustment could be performed in the present methodology.

According to AEDT, the LOS adjustment, LOS_{adj}, is calculated together with the engine installation, $\Delta_I(\phi)$, and the lateral attenuation, $\Lambda(\beta,l)$, for each pair of flight path segment and receiver (for the definitions of Δ_I, Λ, depression angle ϕ, elevation angle β and lateral displacement l see [17]). Then, these values are compared in order to estimate their overall effect through a "lateral correction", LA_{corr}, to be used in the ECAC noise engine:

$$LA_{corr} = \max\left[LOS_{adj}, -\Delta_I(\phi) + \Lambda(\beta, l)\right] \quad (1)$$

The computation of LOS_{adj} requires determining, for each segment-receiver pair, whether the direct sound propagation path is obstructed, and by how much if so. This is done in the present application by comparing the local altitude of the direct propagation path (a simple straight segment connecting flight path and receiver) with the terrain elevation. To account for the terrain, a sample point is taken every about 300 m and its elevation is computed by means of a bilinear interpolation using the four surrounding receiver points. Finally, the differences between local terrain elevation and propagation path altitude are computed, and the maximum value is used to calculate LOS_{adj} according to the AEDT procedure.

2.3 Fleet substitution algorithm

For any assessment of future noise impact from aviation, a major aspect to be taken into account is the change in fleet composition. In fact, when an old aircraft cannot be operated any longer, it is retired and substituted with a newer, generally quieter, model. A fleet substitution algorithm has been developed in the present application to update the aircraft fleet from 2018 to 2025, relying on the ANP database as the source of noise and performance data for the newer aircraft models. The substitution algorithm is split in three steps:

1) identification of the aircraft to be substituted;
2) identification of the substitute aircraft models;
3) assignment of the new model to old flight events.

In the first step, the age of every aircraft at the time of the flight event is recovered using the offline aircraft model database mentioned in Section 2.1.2, and a new database for 2025 is built by increasing the age of each aircraft by 7 years. Then, all aircraft whose age exceeds 22 years are deemed fit for substitution. The cut-off age

derives from a slight simplification of the fleet mix model used for the UK aviation forecasts [22].

The second step consists in deciding which aircraft are best suited to represent the future fleet. In this regard, two aspects must be considered: *i)* while in the next few years new-generation aircraft are expected to dominate the market (e.g. A320neo), some current-generation models are still being sold [23]; *ii)* as the ANP database was last updated in February 2018, some of the new-generation models expected by 2025 are not yet listed, primarily being without official noise certification at the time.

In light of the above considerations, the supply pool containing the substitute aircraft models is built as follows. First, the pool is split into 10 categories according to the aircraft size, represented by maximum weight and approximate number of seats. Second, for each category the aircraft models that are best in class in terms of noise output are identified and retrieved from the first ANP substitution table, and an average configuration for each model is built as explained in Section 2.1.2. The results are listed in Table 1, which also shows that multiple models are chosen for a single category. This is done either because such models have a similar noise output, or to represent better the weight variability within a given category.

The third and final step is the actual fleet modification. Each aircraft fit for substitution is assigned the MTOW of its original ANP proxy, and this parameter is used to identify the supply pool category. The new model is selected randomly except for category < 190,000, where it was decided to preserve the 2018 market split between leading manufacturers Airbus and Boeing by substituting the older aircraft with models from the same company. Note that the selection inside the same category ensures that the old ground track is always compatible with the new aircraft, concerning in particular ground movements and radii of turns.

2.4 Generation of additional flight events

Besides accounting for the aircraft fleet evolution, forecasts of future air traffic scenarios should also consider a possible increase in the number of flight movements. However, while aircraft are retired on an individual basis, the number and characteristics of new flight events depend on multiple factors on global, national and local levels. In the present application, global and national factors are accounted for by using official 7-year EUROCONTROL traffic forecasts [24], which are applied locally to the airport of interest checking whether the predicted increment is compatible with its features and constraints (e.g. maximum runway system capacity).

After selecting an airport and retrieving its expected traffic increase, a flight event generation algorithm is used to create the required number of additional aircraft movements. This algorithm is applied to the events of a single day after the fleet substitution, and makes use of the existing data assets to simulate the traffic increment. It is composed of three steps:

1) separation of existing flight events in 60 sub-classes according to three parameters;
2) retrieval of the number of new flight events in each sub-class;
3) generation of the flight events for each sub-class.

In the first step, the flight events are classified according to the three parameters reported in Table 2. The 60 ($2 \times 10 \times 3$) sub-classes express the traffic split at a given airport, showing which operations are most common for aircraft of a given size during a given part of the 24-h day. This split shows the way the selected airport operates, emphasising inherent restrictions (e.g. avoiding departures of large aircraft at night) that result in zero events registered in some sub-classes. Therefore, introducing the classification in Table 2 enables a strategy for increasing coherently the air traffic at the airport.

Table 1 Supply pool of best-in-class ANP-available aircraft models for the new aircraft fleet in 2025

MTOW [lb]	*Aircraft models*	*Role*	*Seats (approx.)*
< 20,000	Citation CJ4	Business jet	10
< 60,000	EMB 145	Regional jet	50
< 110,000	SSJ100	Regional jet	100
< 140,000	A220–100	Narrow-body airliner	125
< 169,000	A220–300	Narrow-body airliner	150
< 190,000	A320-251 N, A320-271 N, 737 MAX 8	Narrow-body airliner	175
< 220,000	A321-251 N, A321-271 N	Narrow-body airliner	200
< 600,000	787–8, 787–9	Wide-body airliner	275
< 850,000	A350–941, A350–1041	Wide-body airliner	350
> 850,000	A380–841, A380–861	Wide-body 4-engine airliner	> 350

Table 2 Parameters used for classifying existing flight events

Parameter	*Number of classes*	*Description*
Operation type	2	Departure, arrival
Aircraft weight	10	The same as in Table 1
Time of day	3	Day (07:00 to 19:00), evening (19:00 to 23:00), night (23:00 to 07:00)

In the second step, a known percentage of traffic increment is applied to all the 60 sub-classes, and for each of them the number of flight events to be added is found. As these numbers are not integers, all 60 values are floored, and the remaining fractional parts are redistributed across the sub-classes having a number of events closest to an integer. This step implies the assumption that air traffic in 2025 will preserve the split of flight events observed at the selected airport in 2018.

In the third step, the new flight events are generated separately for each sub-class. If m is the number of additional events for a given sub-class, the n events recorded in 2018 for that sub-class are identified, and m among them are randomly chosen and duplicated. This operation, performed across all sub-classes, yields all the events needed to simulate the increased airport traffic.

As a final remark, this algorithm was devised with the sole purpose of computing cumulative noise metrics under forecast traffic scenarios, and therefore does not take into account ATC-related practices such as traffic separation or temporal rearrangement of events for accommodating new flight movements. Possible airport constraints, such as runway system capacity, are duly considered upon application of the algorithm.

3 Results

The noise computation procedure outlined in Section 2.1 and updated to account for the topography of the airport area was applied to the prediction of noise levels due to air traffic in 2025 in three European airports, according to the algorithms of fleet substitution and new flight event generation described in Sections 2.3 and 2.4, respectively. The analysis is based on the flight movement data collected for the previous application [14] in the airports of London Heathrow, Frankfurt, and Vienna-Schwechat. The analysis at Heathrow Airport focuses on the effectiveness of the fleet substitution algorithm, and noise forecasts are validated against official UK noise predictions. At Frankfurt Airport, instead, the effect of an increase in air traffic is added and noise results are compared with their 2018 counterparts. Finally, multiple traffic forecasts are considered for Vienna International Airport, showing the comparative impact of air traffic increment and noise reduction due to quieter aircraft, and the contribution of terrain elevation. Differently from the original application, the dimensions of the 2D grid of receivers were tailored to the airport, but the receiver density was kept unaltered.

3.1 Only fleet substitution: Heathrow airport

Heathrow Airport, located 23 km west of London, is one of the largest airports in the world. It served around 80 million passengers in 2018 with 477,604 aircraft movements [25], causing the current two-runway system to operate near its full capacity of 480,000 movements [22]. Although a third runway is expected to be operative by 2030, the number of movements is unable to increase significantly in the next few years despite the expected air traffic growth in UK [24], which makes this airport a suitable test case for the fleet substitution algorithm.

For Heathrow Airport, official noise forecasts based on 2016 traffic volume and the ANCON model are available [26]. The key cumulative metrics are $L_{Aeq,day}$, $L_{Aeq,night}$ and L_{DEN}, considered for both the average summer 24-h day and the average day of the entire year, and the noise contour area (surface area enclosed by a given contour line) is provided for several noise levels as computed for 2016 and predicted for 2025. Although multiple traffic scenarios for 2025 are considered in the official forecasts, minor differences arise among them, and therefore the so-called "Central Scenario" is chosen as a reference. As for the present calculation, the flight movements on 13 June 2018 (westerly operations) and 11 June 2018 (easterly operations) were updated to 2025 considering fleet renewal but no traffic increase. The resulting noise levels were blended according to a 70%–30% modal split [14] to build single-day cumulative metrics, which are assumed to be representative of both summer average and annual average aircraft noise.

The comparison between official and present predictions is reported in Table 3. The values in km^2 represent the noise contour areas enclosed by the specified contour level. It is worth noting that the traffic increase after 2016 (+ 2.9%) is due to both an actual growth in aircraft movements before 2018 (+ 1.1%) and the flight allocation algorithm used in the official forecasts. This algorithm redistributes the expected countrywide increase in air traffic across all airports, accounting for their residual capacity but forcing the allocation of at least a few additional flights to each airport to ensure algorithm convergence. Concerning noise, as explained in

Table 3 Official and present predictions at Heathrow Airport for 2025

Metric	*Official predictions*			*Present predictions*		
	2016	*2025*	*% change*	*2018*	*2025*	*% change*
Avg. summer day movements	1266.7	1304.3	+ 2.9%	1271.5	1271.5	–
Avg. summer night movements	84.4	86.9	+ 2.9%	79.5	79.5	–
Summer $L_{Aeq,day}$ 51 dB [km^2]	329.4	290.6	−11.7%	180.4	157.7	−12.6%
Summer $L_{Aeq,day}$ 54 dB [km^2]	184.3	166.2	−9.8%	105.1	93.5	−11.0%
Summer $L_{Aeq,night}$ 45 dB [km^2]	193.8	163.7	−15.5%	142.6	124.0	−13.0%
Summer $L_{Aeq,night}$ 48 dB [km^2]	115.2	95.1	−17.4%	87.4	76.1	−12.9%
Annual L_{DEN} 50 dB [km^2]	498.1	436.7	−12.3%	295.6	266.3	−9.9%
Annual L_{DEN} 55 dB [km^2]	198.0	176.0	−11.1%	127.8	111.6	−12.7%
Annual $L_{Aeq,night}$ 45 dB [km^2]	174.8	154.6	−11.6%	142.6	124.0	−13.0%
Annual $L_{Aeq,night}$ 50 dB [km^2]	74.0	59.0	−20.2%	59.9	51.7	−13.7%

the previous paper [14] the present methodology underestimates cumulative levels by 1 to 3 dB. As observed in Table 3, even such small differences can lead to large variations in contour areas for levels as low as 45–55 dB, which are obtained far from the runways where noise decays slowly with distance. However, when examining the relative area changes, a very good agreement is observed between present and official forecasts. In particular, the decrease in contour areas for $L_{Aeq,day}$ and L_{DEN} is predicted quite well, whereas larger deviations are observed for $L_{Aeq,night}$, which is though more susceptible to single flight movements due to the limited number of night-time events.

Figures 2, 3, and 4 show the variations in noise levels, ΔdB, predicted using 6731 receivers that cover a 49-by-24 km^2 airport area. The 2018 noise contours for which contour areas are provided in Table 3 are superimposed on each map. A moderate $L_{Aeq,day}$ decrease is forecast to the north and south-west of the airport, whereas for $L_{Aeq,night}$ significant noise reduction to the south and north-east of it is partially offset by an increment in the south-eastern region. As expected, the map for L_{DEN} shows variations much more similar to $L_{Aeq,day}$. In all cases, the largest changes are mostly far away from the airport, where noise levels are relatively low, whereas an average reduction of around 1 dB is found within the contour areas. Finally, regions in all the three maps are observed where a slight-to-moderate increase in noise levels results from the computation, which is an unexpected occurrence when considering the substitution of old aircraft with newer and quieter ones. In fact, some new aircraft correspond to proxies that are different from those of the retired airplanes, and thus may require different ANP procedures, especially for approach. In particular, some proxies are required to perform a continuous 3° descent from 6000 ft. AGL while others are also prescribed to fly at 3000 ft. AGL for several kilometres, resulting in a longer flight profile and hence in noise increments that are strongest at locations not covered by the shorter procedure.

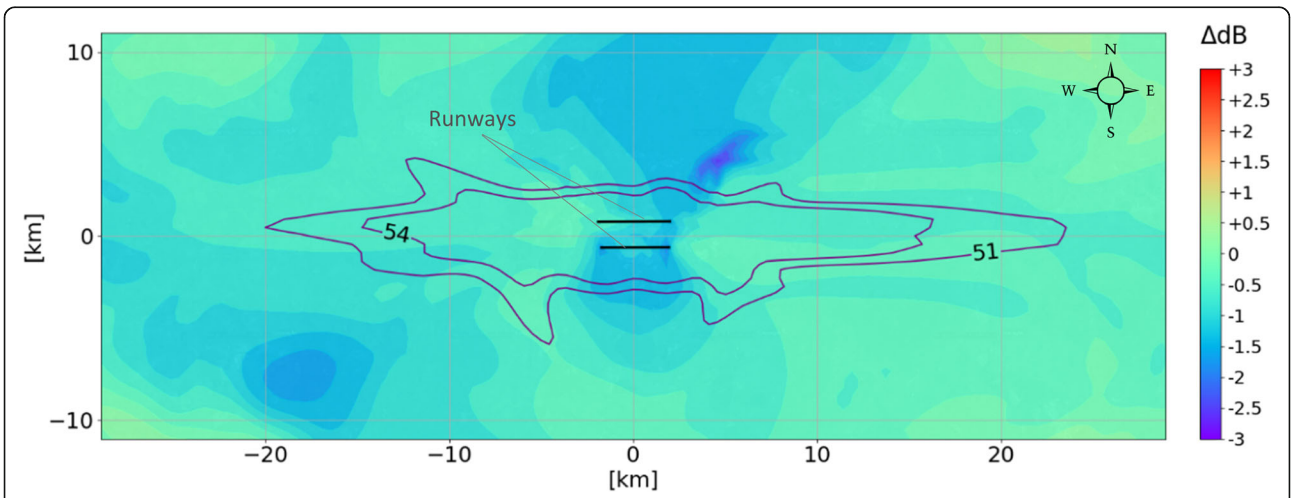

Fig. 2 Map of predicted variations in $L_{Aeq,day}$ at Heathrow Airport from 2018 to 2025 due to fleet substitution ($\Delta dB = L_{Aeq,day,2025} - L_{Aeq,day,2018}$). 51-dB and 54-dB $L_{Aeq,day}$ contour lines computed for 2018 are superimposed

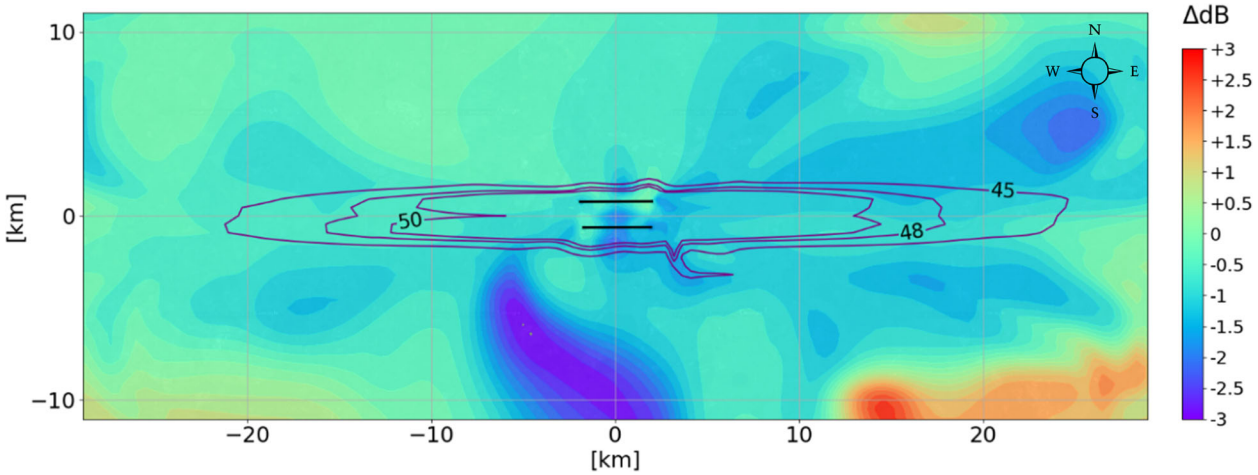

Fig. 3 Map of predicted variations in $L_{Aeq,night}$ at Heathrow Airport from 2018 to 2025 due to fleet substitution ($\Delta dB = L_{Aeq,night,2025} - L_{Aeq,night,2018}$). 45-dB, 48-dB and 50-dB $L_{Aeq,night}$ contour lines computed for 2018 are superimposed

The results above hinge solely on the fleet substitution algorithm, which proves to be successful in light of the following considerations. First, the aircraft age distribution in Fig. 5 shows that about 25% of the airplanes in June 2018 were less than 5 years old, showing a fleet renewal trend that is in line with the substitution of 37% of the aircraft in 7 years provided by the present algorithm. Second, the good predictions of contour area changes in Table 3 are obtained despite the very small number of new aircraft models (see Table 1) compared to the official supply pool [27]. This suggests that the key to carrying out a good prediction is the separation in appropriate aircraft size categories, whereas the number of new aircraft models is much less important if at least one of them is used in each category.

3.2 Fleet substitution and additional flight events: Frankfurt airport

Frankfurt Airport is the largest airport of Germany, with around 69 million passengers served and 512,115 aircraft movements in 2018 [28]. Differently from Heathrow, the four-runway system and the soon-to-be three terminals will be able to handle the future growth in the number of passengers, which is expected to approach 80 million by 2025 [29]. Assuming that average aircraft size and passenger load factors remain unchanged, this forecast is in line with the baseline one from EUROCONTROL, which indicates a 13.9% increase in aircraft movements for Germany in the next seven years. Therefore, this percentage was used in the flight event generation

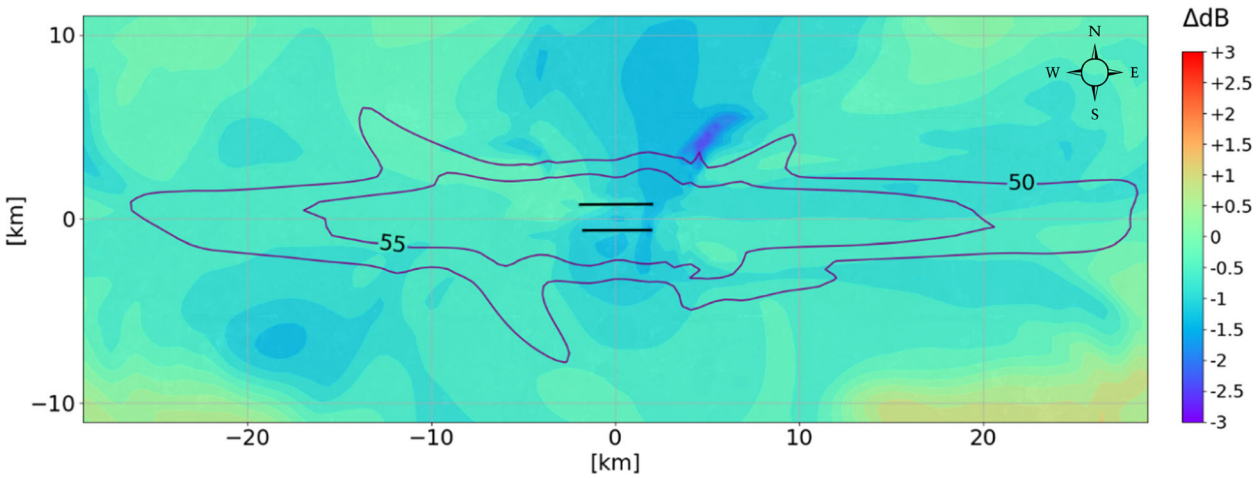

Fig. 4 Map of predicted variations in L_{DEN} at Heathrow Airport from 2018 to 2025 due to fleet substitution ($\Delta dB = L_{DEN,2025} - L_{DEN,2018}$). 50-dB and 55-dB L_{DEN} contour lines computed for 2018 are superimposed

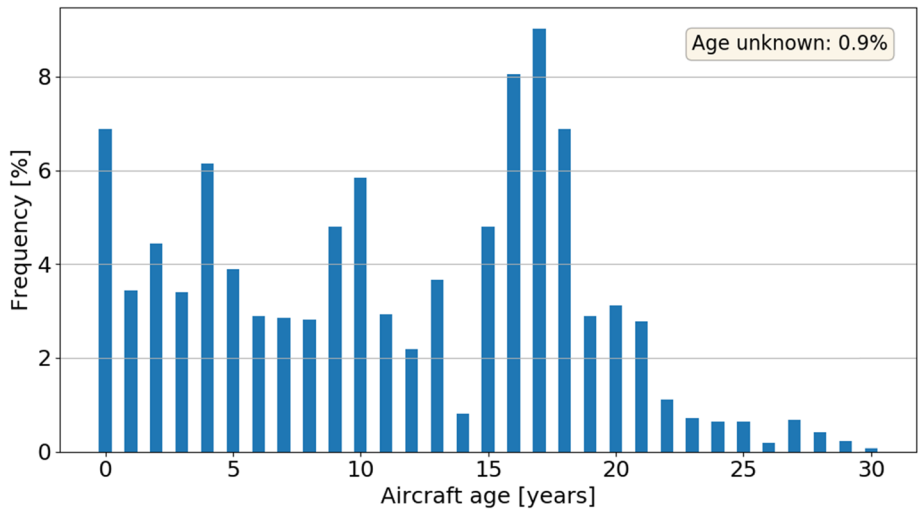

Fig. 5 Age distribution of the aircraft operated at Heathrow Airport on 11 June and 13 June 2018

algorithm, which was applied in conjunction with the fleet substitution one.

Starting from the flight movements collected for 11 June 2018, the computation led to the results reported in Table 4. First, the number of flight movements predicted for 2025 is 1512, which is compatible not only with the planned runway system capacity of 126 movements/h, but even with the current 104 movements/h (Fraport, 2019). Concerning the contour areas, if the fleet substitution is considered without additional movements, the noise reduction is similar to that of Heathrow Airport, although the improvement is slightly lower on average. However, when the traffic increase is considered, the areas become almost as large as in 2018, or even larger in the case of $L_{Aeq,night}$.

The effects of the two contributions on airport noise are shown in Fig. 6, which reports the variations in noise levels, ΔdB, predicted using 10,355 receivers located on a 2200 km^2 airport area. While a simple fleet upgrade causes an overall decrease in noise levels (see Fig. 6(a)), the addition of new flight movements tends to cancel out this improvement (see Fig. 6(b)), leading to very similar 2018 and 2025 L_{DEN} contour sets. As observed and commented for Heathrow, also the ΔdB map in Fig. 6(a) shows some regions where noise increases despite the fleet renewal. These increments are even stronger in Fig. 6(b) due to the contribution of the additional air traffic.

Differently from the case of Heathrow Airport, no official noise forecasts are available for Frankfurt Airport. Therefore, a reasonable justification for the observed trend at Frankfurt is provided on the basis of the following arguments. The considered noise metrics refer to cumulative sound exposure, and exposure scales linearly with flight operations performed by the same aircraft. If E is the sound exposure resulting only from the fleet renewal, the expected sound level increase, ΔL, due to traffic increase ΔI is given by:

Table 4 Air traffic and noise contour areas at Frankfurt Airport in 2018 and 2025, considering or not traffic increase

Metric	*2018*	*2025, no traffic increase*		*2025, with traffic increase*	
	Value	*Value*	*% 7-year change*	*Value*	*% 7-year change*
16-h-day movements	1234	1234	–	1406	+ 13.9
8-h-night movements	95	95	–	106	+ 11.6(*)
$L_{Aeq,day}$ 52 dB [km^2]	157.6	141.3	−10.3	156.8	−0.5
$L_{Aeq,day}$ 57 dB [km^2]	67.0	59.0	−11.9	64.6	−3.6
$L_{Aeq,night}$ 47 dB [km^2]	115.2	108.3	−6.0	117.0	+ 1.6
$L_{Aeq,night}$ 52 dB [km^2]	42.3	37.6	−11.1	42.7	+ 0.9
L_{DEN} 55 dB [km^2]	140.6	129.0	−8.2	140.8	+ 0.1
L_{DEN} 60 dB [km^2]	55.4	48.4	−12.0	54.8	−1.1

(*) less than 13.9% due to the flooring in the flight event generation algorithm

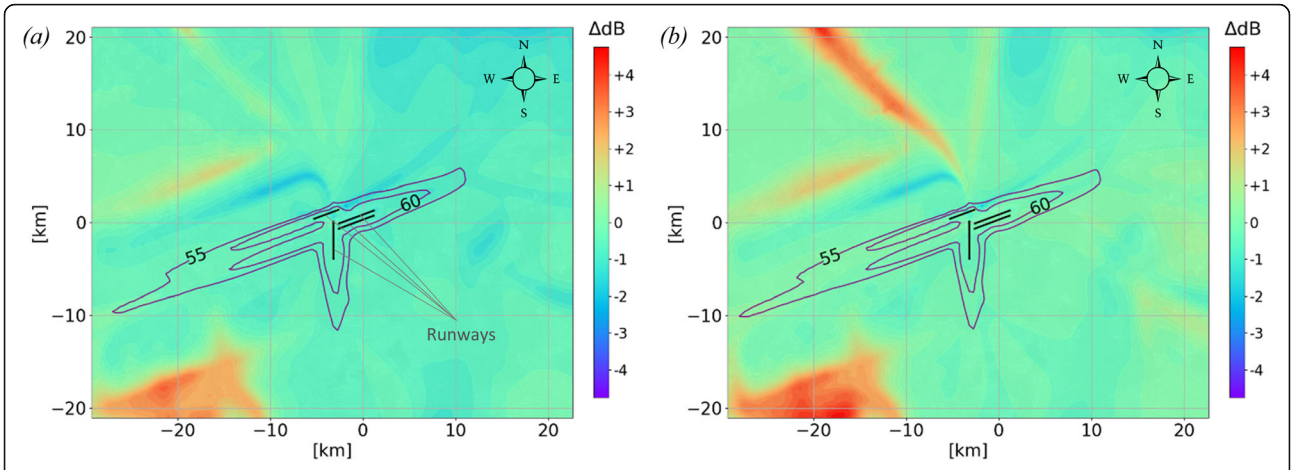

Fig. 6 Maps of predicted variations in L_{DEN} at Frankfurt Airport from 2018 to 2025 ($\Delta dB = L_{DEN,2025} - L_{DEN,2018}$). **a** Effect of fleet substitution, 2018 L_{DEN} contours. **b** Effects of fleet substitution and traffic increase, 2025 L_{DEN} contours

$$\begin{aligned} \Delta L &= 10\ \log_{10}(E\cdot(1+\Delta I)) - 10\ \log_{10}(E) \\ &= 10\ \log_{10}(1+\Delta I) \end{aligned} \quad (2)$$

With a 13.9% traffic increase, the expected ΔL is 0.565 dB. In fact, the average increments for metrics $L_{Aeq,day}$, $L_{Aeq,night}$, and L_{DEN} range from 0.54 to 0.59 dB, showing that the present algorithm yields good results as long as the additional movements generate the same average noise emissions as the original flight events.

3.3 Multiple traffic forecasts: Vienna international airport

As shown in the previous subsection, an increase in traffic volume at a given airport is liable to offset the decrease in noise levels due to the entry into service of new-generation aircraft. The relation between these two effects is examined in more detail at Vienna International Airport (also known as Vienna-Schwechat Airport or Vienna Airport), which is the largest airport of Austria with two runways and about 27 million passengers served in 2018 [30]. With reference to the flight movements collected for 10 June 2018, three EUROCONTROL traffic forecasts for Austria, namely "Low", "Baseline", and "High", were used to discover how much traffic increment is sustainable without worsening noise levels around the airport.

Since three different traffic forecasts needed considering, the fleet substitution was performed only once, but the generation of additional flight events was repeated three times with the appropriate increments. A preliminary check showed that the runway system capacity of 74 movements/h is large enough to accommodate all events even in the worst case of "High" scenario. The results for L_{DEN} are reported in Table 5, where an upward trend in contour areas is observed as the number of flight movements increases. The relative changes in contour areas are linearly regressed in the plot of Fig. 7 for the three different sets of L_{DEN} values, showing that the increase in traffic volume necessary to cancel out the improvements due to fleet substitution is about 23%. This value is not only higher than the most likely "Baseline" traffic forecast, but also well above the – 2.1% registered from 2011 to 2018 [30], suggesting that aircraft noise might not be the worst problem for the airport to face in the short term. However, the situation may change if a third runway is built [31], as the expanded airport capacity could lead to an unpredictably large increase in flight movements.

The variation of L_{DEN} in the airport area is examined in Fig. 8, which shows the effects of sole fleet renewal without additional movements and the three traffic scenarios. The predictions refer to an area of about 2075 km^2 covered with 9898 receivers. As expected under the current assumptions, the contour areas grow keeping almost the same shape as the traffic volume increases, but it is worth noting that under the "High" scenario in

Table 5 L_{DEN} at Vienna in 2018 and 2025 under four assumptions (N = no traffic increase, L = low, B = baseline, H = high)

Metric	*2018*	*2025, N*		*2025, L*		*2025, B*		*2025, H*	
	Value	*Value*	*% change*	*Value*	*% change*	*Value*	*% change*	*Value*	*% change*
Flight movements	710	710	–	767	+ 8.0	848	+ 19.4	907	+ 27.7
L_{DEN} 45 dB [km^2]	323.4	280.5	−13.3	293.9	−9.1	319.9	−1.1	333.6	+ 3.2
L_{DEN} 50 dB [km^2]	134.8	118.1	−12.4	123.4	−8.5	133.5	−1.0	138.9	+ 3.0
L_{DEN} 55 dB [km^2]	56.7	49.3	−13.1	51.9	−8.5	53.5	−5.6	59.2	+ 4.4

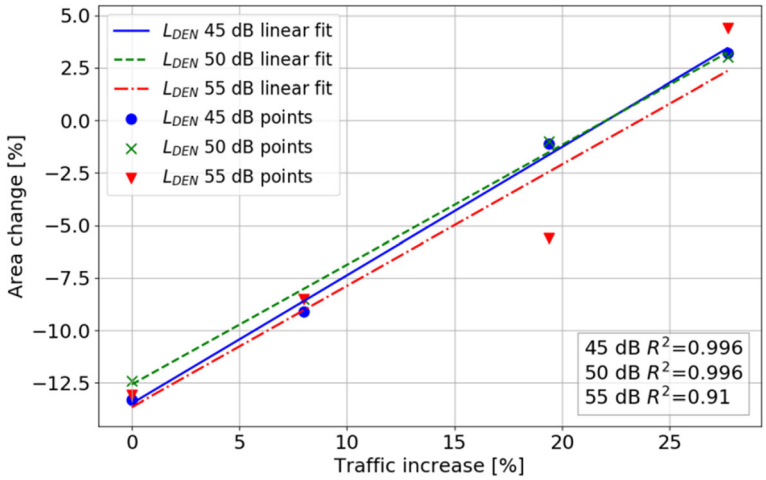

Fig. 7 Linear regression of the contour area changes for the L_{DEN} values listed in Table 5

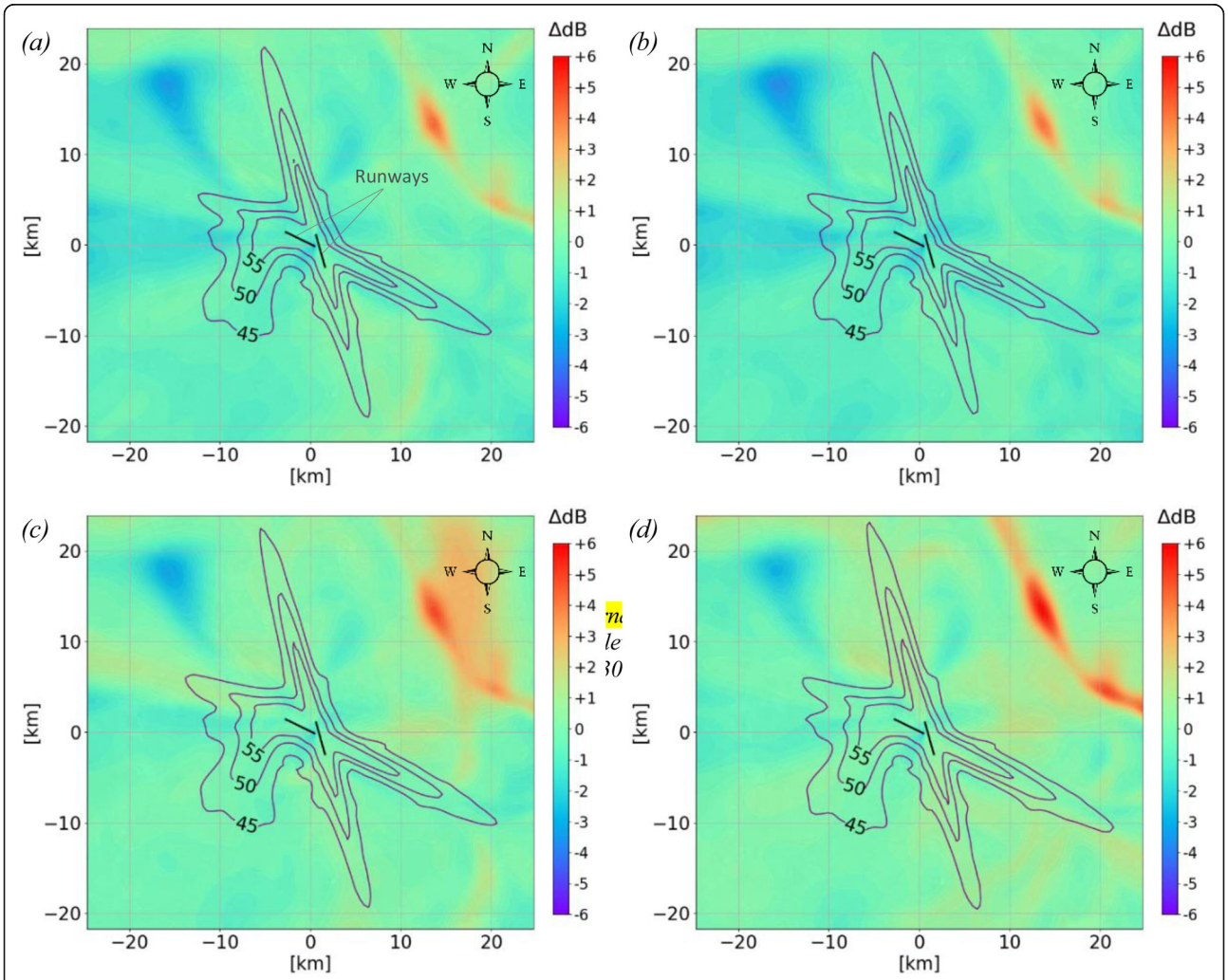

Fig. 8 Maps of predicted variations in L_{DEN} from 2018 to 2025, and 2025 L_{DEN} contours at Vienna International Airport for (**a**) unaltered traffic volume, (**b**) low increase, (**c**) baseline increase, (**d**) high increase ($\Delta dB = L_{DEN,2025} - L_{DEN,2018}$). Fleet substitution is applied in all the four cases

Fig. 8(d) there is a slight increase in noise (close to 1 dB) also outside the narrow strips along the typical arrival and departure routes.

Similarly to Frankfurt Airport, markedly higher noise levels due to both different approach procedures and traffic increase can be observed locally (e.g. north-east of the runways).

Finally, since Vienna International Airport lies close to the Alps, its hilly surroundings enable a meaningful analysis of the influence of topography on noise levels. In general, the introduction of terrain features both alters the elevation of the runways and causes a vertical displacement of the sound receivers. The maps of L_{DEN} and $L_{max,avg}$ variations in Fig. 9 show that the combination of these two effects at Vienna Airport leads to a slight reduction in the noise levels along most of the aircraft routes when compared to previous results obtained for flat terrain at ARP elevation [14]. However, in the vicinity of the most elevated regions, L_{DEN} rises by up to 2 dB, as shown in Fig. 9(a). This increase occurs primarily because the receivers are closer to the flying aircraft, and thus the average distance between path segments and sound receivers decreases. The along-route reduction and local increment in noise levels are intensified when considering metrics based on maximum sound levels, such as $L_{max,avg}$ in Fig. 9(b), because these ones, instead of depending on cumulative exposure from all flight path segments, are dominated by the noisiest path segment of each flight event. As the noisiest segment is usually the closest to the sound receiver, terrain elevation becomes a considerable fraction of this segment-receiver distance, leading to a stronger reduction in the along-route noise but causing local increments to approach or exceed 3 dB, as detected to the south and north-west of the airport.

4 Conclusions

The approach presented in this paper is an evolution of the original methodology devised by the authors [14] for the computation of noise in airport areas based on ECAC noise model and Internet-based information sources. Besides accounting for the topographic features of the airport area, the present approach introduces two algorithms for aircraft fleet renewal and reconstruction of new flight events, which are used to forecast airport noise according to future air traffic scenarios. Predictions of noise contours for 2025 have been carried out for three large European airports (London Heathrow, Frankfurt, Vienna-Schwechat), focusing on fleet renewal at Heathrow, air traffic increase at Frankfurt, and multiple traffic scenarios at Vienna-Schwechat.

Data from digital elevation models have been collected, processed into usable terrain elevation maps, and implemented into the noise computation methodology. In particular, the addition of line-of-sight blockage to the ECAC noise engine enables accounting for the shielding effect due to terrain features. The two algorithms for fleet substitution and generation of new flight events use and readapt, under reasonable assumptions, historical data on flight movements, aircraft models and airports. The key merit of these algorithms is the classification of the current aircraft fleet into 10 size categories, which allows performing a coherent redistribution of new aircraft and

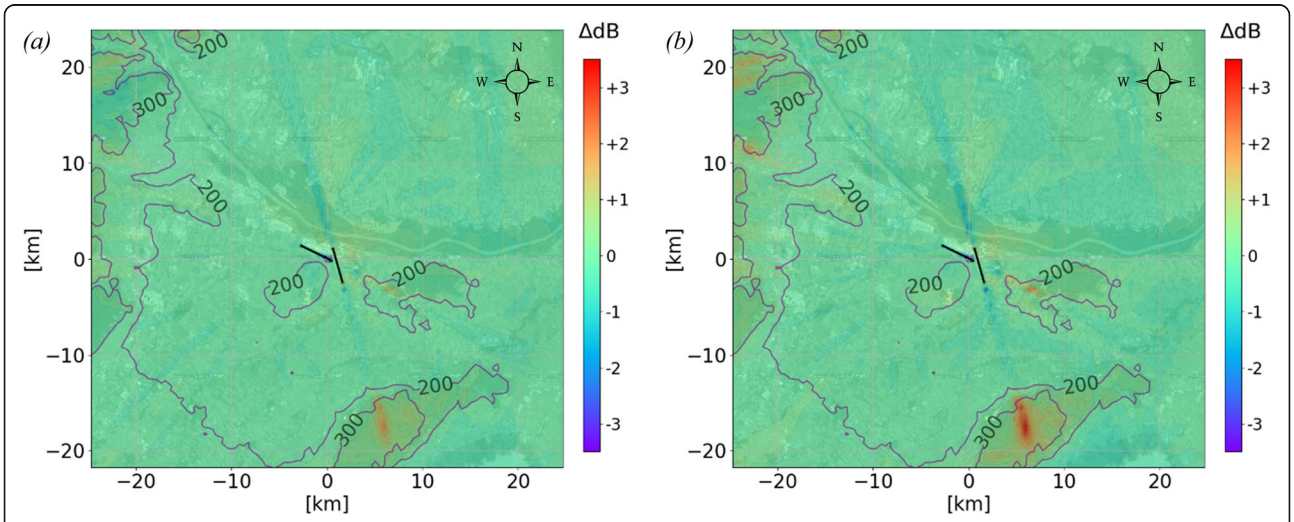

Fig. 9 Variations in L_{DEN} (a) and $L_{max,avg}$ (b) at Vienna International Airport in 2018 due exclusively to the implementation of terrain elevation data, without fleet substitution (**Δ**dB = level considering elevation − level considering flat terrain). The elevated regions (above 200 or 300 m) are enclosed by contour lines

flight events in the same categories to model future air traffic scenarios. The forecasts for Heathrow Airport show that the fleet substitution algorithm is able to provide reliable estimates of the relative changes in noise levels, while reasonable results have been obtained for Frankfurt Airport when considering also an increase in flight movements. The analysis of multiple traffic scenarios at Vienna International Airport has allowed identifying the air traffic volume that balances the noise increase from additional flight events with the use of quieter aircraft. Finally, the effect of terrain elevation around Schwechat results in a modest variation in the exposure-based noise metrics, while the maximum levels in the most elevated regions increase by more than 3 dB.

The present application allows forecasting airport noise by rearranging past and present publicly available web data to simulate future air traffic scenarios for any civil airport in the world. Therefore, it represents a widely usable and general approach, the main limitation of which remains a moderate underestimation of the absolute noise levels, as explained by Pretto et al. [14]. In addition, this procedure is quite flexible, as changes can be easily made to account for other new-generation aircraft (once officially certified) and different MTOW distributions for future aircraft fleets, while sensitivity analyses can be carried out via simple modification of parameters such as traffic increment or maximum aircraft age. All these aspects make the present application a lean and powerful tool for assessing changes in airport noise under different future scenarios, and, as such, very well suited for aviation policy-makers.

5 Nomenclature

All symbols in the equations are defined in the text.

Acronyms

ADS-B Automatic Dependent Surveillance – Broadcast
AEDT Aviation Environmental Design Tool
AGL Above Ground Level
ANCON Aircraft Noise Contour [Model]
ANP Aircraft Noise and Performance
ARP Airport Reference Point
ATC Air Traffic Control
CAA Civil Aviation Authority
DEM Digital Elevation Model
ECAC European Civil Aviation Conference
EU European Union
FAA Federal Aviation Administration
ICAO International Civil Aviation Organization
LOS Line-Of-Sight
MTOW Maximum Take-Off Weight
NPD Noise-Power-Distance
UK United Kingdom

Noise metrics

SEL A-weighted sound exposure level generated by a single flight event.
L_{Amax} Maximum A-weighted sound level generated by a single flight event.
$L_{Aeq,W}$ Time-weighted equivalent sound level. It is the level of the average sound intensity due to N flight events during measurement period T_0. Time-of-day weighting factor Δ_i is added to single event level SEL_i to account for increased noise annoyance during evening and night. The time-weighted level is calculated as follows:

$$L_{Aeq,W} = 10\log_{10}\left(\frac{1}{T_0}\sum_{i=1}^{N}10^{(SEL_i+\Delta_i)/10}\right)$$

From this expression, the three cumulative noise metrics below are defined.

$L_{Aeq,day}$ 16-hour day-average sound level. T_0 = 57,600 s (07:00-23:00) and Δ_i = 0 dB.
$L_{Aeq,nigh}$ 8-hour night-average sound level. T_0 = 28,800 s (23:00-07:00) and Δ_i = 0 dB.
L_{DEN} Day-evening-night average sound level. T_0 = 86,400 s, Δ_i = 5 dB in the evening (19:00-23:00), Δ_i = 10 dB at night (23:00-07:00), Δ_i = 0 dB otherwise.
$L_{max,avg}$ Average maximum sound level. It is calculated as follows:

$$L_{max,avg} = 10\log_{10}\left(\frac{1}{N}\sum_{i=1}^{N}10^{L_{Amax,i}/10}\right)$$

where $L_{Amax,i}$ if the maximum level of the i-th flight event and N is the number of events.

Acknowledgements
Not applicable.

Authors' contributions
MDG, MP and PG conceived the work, identified the key focus points, and defined the scenarios to be analysed. Under PG's supervision, MP devised and implemented the algorithms for fleet substitution and flight event generation, besides applying DEMs to account for the topography of airport areas. The results were obtained by MP and analysed by MP and PG, who also drafted the manuscript. MDG, AZ and HK provided a significant contribution towards the overall revision of the manuscript and the improvement of the data/results rendering format. All authors approved the paper.

Funding
Not applicable.

Availability of data and materials
Flight tracking data from *FlightAware* are available from the corresponding author on reasonable request. Aircraft model databases, airport data, and DEMs are available on websites *Airlinerlist*, *OurAirports*, and *WebGIS*, respectively. The ANP database is accessible upon permission from EUROCONTROL.

Competing interests
The authors declare that they have no competing interests.

Author details
[1]Dipartimento Politecnico di Ingegneria e Architettura, University of Udine, Via delle Scienze 206, 33100 Udine, Italy. [2]AIT Austrian Instutute of Technology GmbH, Center for Low-Emission Transport, Giefinggasse 2, 1210 Vienna, Austria.

Received: 3 July 2019 Accepted: 3 December 2019

References

1. ICAO. (2019). *Presentation of 2017 Air Transport Statistical Results.* Retrieved April 17, 2019, from https://www.icao.int/annual-report-2017/Pages/the-world-of-air-transport-in-2017-statistical-results.aspx
2. EUROCONTROL. (2018). *European Aviation in 2040 - Challenges of Growth.* Retrieved April 2, 2019, from https://www.eurocontrol.int/articles/challenges-growth
3. Jimenez, E., Claro, J., Pinho de Sousa, J., & de Neufville, R. (2017). Dynamic evolution of European airport systems in the context of low-cost carriers growth. *Journal of Air Transport Management, 64*, 68–76. https://doi.org/10.1016/j.jairtraman.2017.06.027.
4. European Commission. (2011). Flightpath 2050 - Europe's vision for aviation. *Publications Office of the European Union*. https://doi.org/10.2777/50266.
5. Grampella, M., Lo, P. L., Martini, G., & Scotti, D. (2017). The impact of technology progress on aviation noise and emissions. *Transp Res A, 103*, 525–540. https://doi.org/10.1016/j.tra.2017.05.022.
6. Baharozu, E., Soykan, G., & Ozerdem, M. B. (2017). Future aircraft concept in terms of energy efficiency and environmental factors. *Energy, 140*, 1368–1377. https://doi.org/10.1016/j.energy.2017.09.007.
7. Staples, M. D., Suresh, P., Hileman, J. I., & Barrett, S. R. (2018). Aviation CO2 emissions reductions from the use of alternative jet fuels. *Energy Policy, 114*, 342–354. https://doi.org/10.1016/j.enpol.2017.12.007.
8. Filippone, A. (2014). Aircraft noise prediction. *Progress in Aerospace Sciences, 68*, 27–63. https://doi.org/10.1016/j.paerosci.2014.02.001.
9. Flightradar24. (2019). https://www.flightradar24.com/. Retrieved April 4, 2019
10. FlightAware. (2019). https://flightaware.com/. Retrieved April 3, 2019
11. European Commission. (2017). Commission implementing regulation (EU) 2017/386 of 6 March 2017 amending implementing regulation (EU) no 1207/2011 laying down requirements for the performance and the interoperability of surveillance for the single European sky. *Official Journal of the European Union, 60*, 34–36.
12. Sun, J., Ellerbroek, J., & Hoekstra, J. M. (2019). WRAP: An open-source kinematic aircraft performance model. *Transportation Research Part C, 98*, 118–138. https://doi.org/10.1016/j.trc.2018.11.009.
13. De Gennaro, M., Zanon, A., Kuehnelt, H., Pretto, M., & Giannattasio, P. (2018). Big data for low-carbon transport: an overview of applications for designing the future of road and aerial transport. *7th European Transport Research Arena 2018*. Vienna. https://doi.org/10.5281/zenodo.1440969.
14. Pretto, M., Giannattasio, P., De Gennaro, M., Zanon, A., & Kühnelt, H. (2019). Web data for computing real-world noise from civil aviation. *Transportation Research Part D, 69*, 224-249. https://doi.org/10.1016/j.trd.2019.01.022.
15. European Civil Aviation Conference. (2016a). *Doc 29: Report on Standard Method of Computing Noise Contours around Civil Airports* (4th ed., Vol. 1: Applications guide). Retrieved November 2, 2017, from https://www.ecac-ceac.org/ecac-docs
16. EUROCONTROL. (2019). *The Aircraft Noise and Performance (ANP) Database : An international data resource for aircraft noise modellers*. Retrieved March 5, 2019, from https://www.aircraftnoisemodel.org/
17. European Civil Aviation Conference. (2016b). *Doc 29: Report on Standard Method of Computing Noise Contours around Civil Airports* (4th ed., Vol. 2: Technical guide). Retrieved November 2, 2017, from https://www.ecac-ceac.org/ecac-docs
18. OurAirports. (2019). http://ourairports.com/. Retrieved February 22, 2019
19. Airlinerlist. (2019). http://www.planelist.net/. Retrieved April 2, 2019
20. WebGIS. (2019). http://www.webgis.com/. Retrieved February 27, 2019
21. Federal Aviation Administration. (2017). *Aviation Environmental Design Tool (AEDT) Version 2d, Technical Manual.* Retrieved January 15, 2019, from https://aedt.faa.gov/2d_information.aspx
22. Department for Transport. (2017). *UK Aviation Forecasts.* Retrieved March 15, 2019, from https://www.gov.uk/government/publications/uk-aviation-forecasts-2017
23. Airbus. (2019). *Orders and Deliveries - The month in review: March 2019.* Retrieved April 13, 2019, from https://www.airbus.com/aircraft/market/orders-deliveries.html
24. STATFOR Team. (2019). *EUROCONTROL Seven-Year Forecast February 2019.* EUROCONTROL. Retrieved April 2, 2019, from https://www.eurocontrol.int/publications/seven-year-forecast-feb-2019
25. CAA. (2019). Airport data 2018. Retrieved March 27, 2019, from https://www.caa.co.uk/Data-and-analysis/UK-aviation-market/Airports/Datasets/UK-Airport-data/Airport-data-2018/
26. Environmental Research and Consultancy Department. (2019). *Aviation Strategy: Noise Forecast and Analyses - Version 2.* Civil Aviation Authority. Retrieved March 13, 2019, from http://publicapps.caa.co.uk/modalapplication.aspx?appid=11&mode=detail&id=8958
27. Ricardo Energy and Environment. (2017). *A Review of the DfT Aviation Fleet Mix Model.* Retrieved March 18, 2019, from https://www.gov.uk/government/publications/dft-aviation-fleet-mix-model-a-review
28. Fraport AG. (2019a). *Monthly Traffic Results Frankfurt Airport.* Retrieved April 11, 2019, from https://www.fraport.com/content/fraport/en/our-company/investors/traffic-figures.html
29. Fraport AG. (2019b). Visual Fact Book 2018. Retrieved April 11, 2019, from https://www.fraport.com/content/fraport/en/our-company/investors/events-und-publications/publications/visual-fact-book.html
30. Vienna International Airport. (2019). *Traffic results.* Retrieved April 15, 2019, from https://www.viennaairport.com/en/company/investor_relations/news/traffic_results
31. Flughafen Wien AG. (2011). Zukunft Flughafen 3. Piste. Retrieved April 8, 2019, from https://www.viennaairport.com/en/company/flughafen_wien_ag/third_runway_project

Publisher's Note